

# AN INVESTIGATION ON THE EFFECT OF ASPECT RATIO VARIATIONS ON INDUCED DEFORMATION MODES OF SELF-REINFORCED POLYPROPYLENE COMPOSITE AT ROOM TEMPERATURE

N. A. Zanjani<sup>1\*</sup>, S. Kalyanasundaram<sup>1</sup>

<sup>1</sup>*School of Engineering, Australian National University, North Road, Canberra 0200, Australia*

\* *nima.akhavan@anu.edu.au*

**Key words:** Woven Thermoplastic Composite Material, Forming Limit Diagram, Stamp Forming, Real Time Strain Measurements

## Abstract

*A feasibility study of stretch forming has been investigated in this work on Woven Thermoplastic Composites. Formability characteristics during stamp forming in terms of principle strains were carried out through a Real Time Strain Measurement System. Composite samples with different aspect ratios were utilized to generate different forming modes by clamping in a custom built lock ring and formed to failure by a hemispherical punch. By employing various geometries, different strain states were induced in the sheets. The outcome of these experiments comprised a Forming Limit Diagram (FLD) which elucidated the safe deformation margins for self-reinforced polypropylene (All-PP) woven composites.*

## 1 Introduction

Composite materials offer a wide range of improved benefits over other materials. These include a high strength-to-volume ratio, improved wear resistance and high energy absorption. The substitution of metallic parts with composite materials can provide a weight reduction of 10% to 50% and a cost reduction of 10% to 20% while maintaining similar mechanical properties [1]. Despite these characteristics, drawbacks are evident which are specifically related to the current composite manufacturing technologies such as Liquid Composite Molding (LCM) and curing using an autoclave[2]. Most of the current manufacturing technologies are labor intensive and complex in nature which makes the manufacturing process time consuming and the final part expensive. Thus the applications of these advanced materials have been restricted to low volume aerospace applications.

Thermoplastic composites can be re-shaped after they are initially consolidated by high temperature processes. This behavior makes them better candidates than thermosets for mass production. Thermoplastic composites are currently used in several automotive applications such as front-end panels, spare wheel wells, underbody closures, and door panels [3]. The developments of structural parts made from woven composites are increasing in recent times. Woven composites offers improved damage tolerance due to interlacing tows which can resist well against crack propagation [4]. The other beneficial aspects of woven composites lie in their excellent integrity and balanced in-plane mechanical and thermal properties [5]. Thus, the superior mechanical properties of thermoplastic composites present an opportunity for the

widespread use of these material systems for automotive applications. Cabrera et al. [6] investigated hot compaction process and direct stamping method and their feasibility for production of self-reinforced thermoplastic composites. Lee et al. [7] and Lim et al. [8] investigated glass fiber reinforced polypropylene at elevated temperatures employing a dome-shaped punch. Results were presented on interaction between stretch and draw behavior of Woven Thermoplastic Composite Material (WTPCM) sheets. In addition, the effects of punch speed, forming temperature and glass fiber volume fraction on the induced strain ratios were studied. R.H.W Thije et al. [9] investigated friction between thermoplastic composite laminates and forming tool. Q. Chen et al. [10] and F. Abbassi et al. [11] investigated thermoforming of woven thermoplastic composites. They studied mechanisms influencing forming behavior of WTPCM. B. Zhu et al. [12] investigated formability of commingled E-glass and Polypropylene (PP) woven composites during stamping of prepreg composite sheets by a cone-shaped punch at room temperature.

Stamp forming has been preliminary applied on metals as a rapid production technique and extensive research has been conducted in this area [13]. This process involves forming of material blanks rapidly by a punch and its conforming die. The production costs of final products are inexpensive due to high production rate and long life of the equipment. Furthermore high quality parts are easily achievable. As a result, this method is extensively applied in various industries. In order to implement stamp forming method on sheets to get flawless parts an approach based on Forming Limit Diagram (FLD) is often adopted. The process involves forming of different parts up to the failure depth. Based on the geometry, each of the samples will fail in a specific mode of deformation which is distinguished by a different major-to-minor strain ratio. From different experiments, this ratio is extracted and specified in strain space which finally results in the FLD. This diagram represents formability of the material in the strain space, above which the material fails. For various types of metals and metallic alloys, FLD diagrams have been extracted and studied extensively [13]. However, application of this technique on composites is still very rare. A. Sexton et al. [14] studied stretch forming of Fibre Metal Laminates (FML) with seven different geometries. Based on the results, it was concluded that FML exhibited better formability than Al in terms of strain ratio which was due to the wider forming envelope. L. Mosse et al. [15-18] studied stamp forming of FMLs both experimentally and numerically. C. Morrow et al. [19] investigated stretch forming behavior of pre-consolidated self-reinforced polypropylene (SRPP) thermoplastic composites at room temperature. It was found out that SRPP composite sheets offer superior formability comparing to sheet metals at room temperature due to their capacity to sustain larger minor strain for given major strain.

This work investigates the formability of pre-consolidated rectangular sheets made of all-PP polypropylene woven composite under stamp forming. The objective of this research is to study the effect of dimensional aspect ratios of rectangular specimens on different deformation modes induced by a hemispherical punch. By acquiring samples with different length-to-width ratios, different deformation modes from biaxial deformation up to uniaxial stretch have been observed.

## **2 Experimental Procedure**

### *2.1 Material*

Specimens were made of polypropylene self-reinforced woven composite, CURV™, produced by Propex Fabrics of Germany. It is initially composed of balanced twill-weave polypropylene fabric impregnated in polypropylene resin, consequently processed in a heat compaction procedure to produce final consolidated bi-directional sheets. These sheets are

light-weight (approximately 0.9 g/cm<sup>3</sup>) and fully recyclable.

### 2.2 Specimens geometries

Different methods have been proposed to obtain FLD for different type of materials. These methods take advantage of variation in a key parameter to induce different deformation modes during deformation of the samples. These include change in frictional conditions between samples and punch, change in blank holder force and varying geometries. By employing specimens with different geometrical dimensions, the amount of material to be deformed will change and therefore different pre-failure strains will be achieved. The specimens used for stamping in this study were rectangular in shape acquiring different length-to-width ratios. Their dimensions are summarized in table 1. All of the specimen lengths and thicknesses were equal to 200 mm and 1 mm respectively.

Sample	Width (mm)
Re1W12.5	12.5
Re2W25	25
Re3W50	50
Re4W75	75
Re5W100	100
Re6W125	125
Re7W150	150
Re8W200	200

Table 1. Specimens dimensions

### 2.3 Experimental setup

The stretch forming process was accomplished by a 300 kN custom-build stamping press equipped with a 100 mm in diameter hemispherical punch and a 105 mm open die. Blank holder and die dimensions are shown in figure 1. Data acquisition and press parameters control (feed rate and punch displacement) were accomplished through a local PC. A load cell was also employed to measure the punch force versus displacement of the punch. Six M12 bolts were used to completely fix the specimens in the fixture.

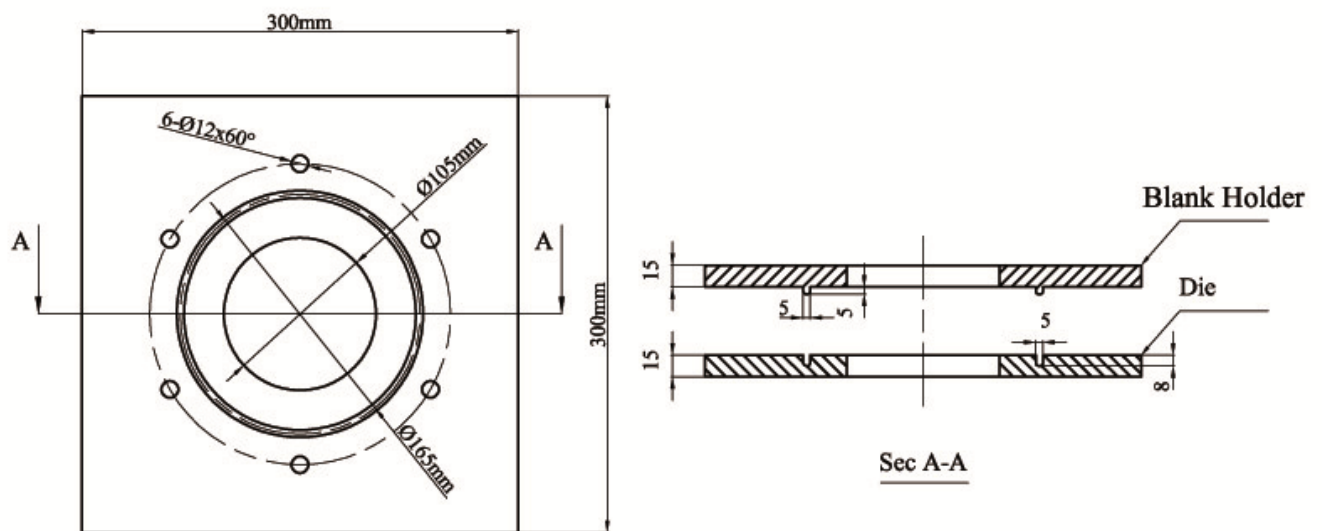


Figure 1. Die and Blank holder drawing

In order to prevent samples to pre-fail in the lock ring region and to let the samples deform up to the maximum possible depth, samples with less than 100 mm width were fixed with a 15 kN.m tightening torque and the rest were tightened with 30 kN.m torque. The procedure started with surface spray of the samples by a stochastic pattern of dots. Afterwards they were clamped in the fixture equipped with the lock ring. The fixture and the sample were then taken to the press and deformed by the punch with a 10 mm/sec feed rate up to the depth of failure. Occurrence of failure was spotted by a sudden drop in the punch load. The principle strains and their evolution were captured and recorded by a 3D photogrammetric measurement system (ARAMIS) under the open die by a T-Junction. The shutter speed was selected equal to 20 frames per second which resulted in taking approximately 10 pictures of the deformed specimen for each 5 mm depth of punch penetration. Startup of the ARAMIS system was triggered by a signal sent from the punch when it started its downward movement.

### 3 Results and discussions

All samples with different geometries were mechanically tested by the custom-built stamping press. The maximum downward punch displacement was set to 60 millimeter to ensure each sample would reach failure.

#### 3.1 Punch force and displacement

Force - displacement diagram is presented in figure 2. The vertical axis represents punch force to deform the specimens up to the desired depth and the horizontal axis represents vertical displacement of the punch. This diagram reveals mechanical behavior of SRPP during stamping process. The maximum force represents failure point of the specimens. Failure for SRPP samples is marked by a consequent drop in the punch force.

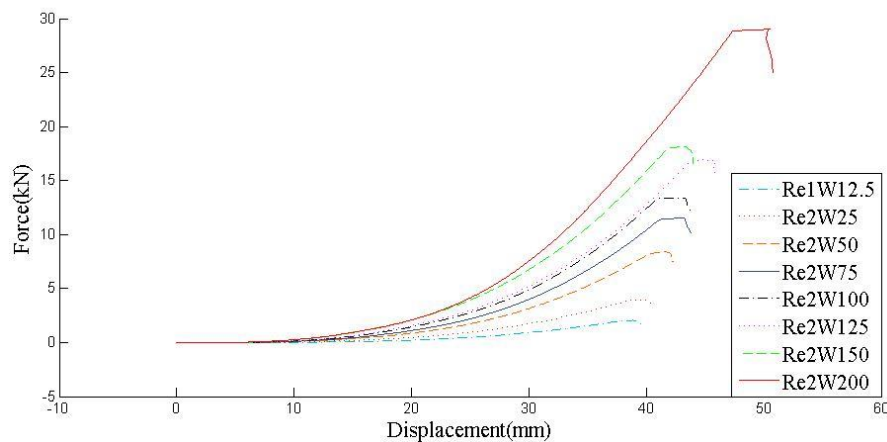


**Figure 2.** Force-Displacement diagram for different geometries

It can be observed that as the geometries become wider, the force required to fracture those increases. The wider samples require more energy to de-bond polymeric chains and to make the samples to fail. It can be observed, from the figure 2, that force required to fracture Re8W200 sample, the widest sample, is 29kN while for Re1W12.5 specimen, the thinnest sample, it only reaches to 2kN. Notably, necking cannot be observed in stretch forming of SRPP which is a common phenomenon during sheet metal forming procedure. This is not only confirmed by the visual observation of the samples after failure, but also could be validated by the force-displacement diagram as force drops rapidly. This suggests that failure of SRPP is an abrupt process accompanied by a sudden dissipation of energy. Therefore, exact determination of FLD for SRPP and similar composites is crucial to predict mechanical response of this class of material under stretch forming conditions, as no obvious sign exist

prior to failure. It is also evident that, smaller samples respond more gradually to stretching than bigger ones. Stretch forming behavior of Re1W12.5 can be approximated by a linear line whilst for wider specimens the punch force varies in a parabolic manner. The last observation is related to the punch force drop of samples after failure. Apparently, the smaller samples fail smoothly and the force drops gradually after failure. On the other hand, the wider samples experience a very sharp drop in force-displacement diagram. This can be explained by the accumulation of energy required for large deformations of wider samples and subsequent catastrophic energy release due to failure of the fibres.

### 3.2 Pole strain Evolution

Application of ARAMIS system enables us to capture strains and their evolution during all stages of stretch forming. In order to compare behavior of samples during stamping procedure and to track their strain state during deformation, the behavior of their poles (the center of the samples) has been studied. The major and minor pole strain evolution of different geometries during stretch forming is presented in figure 3. These deformation modes vary between biaxial strain, plain strain and uniaxial strain. The wider samples experience biaxial mode which is due to their fully clamped boundaries, yet existence of enough material to flow into the mold cavity. This causes the pole to be extended in principal directions, therefore enforces the biaxial strain state to govern the deformation behavior of the pole. On the other hand, smaller samples are clamped only at two opposite edges, by considering small amount of material exists in these thin strips, they experience only uniaxial extension mode. The plain strain deformation is related to the samples not fully clamped, acquiring enough material to flow into the die cavity.

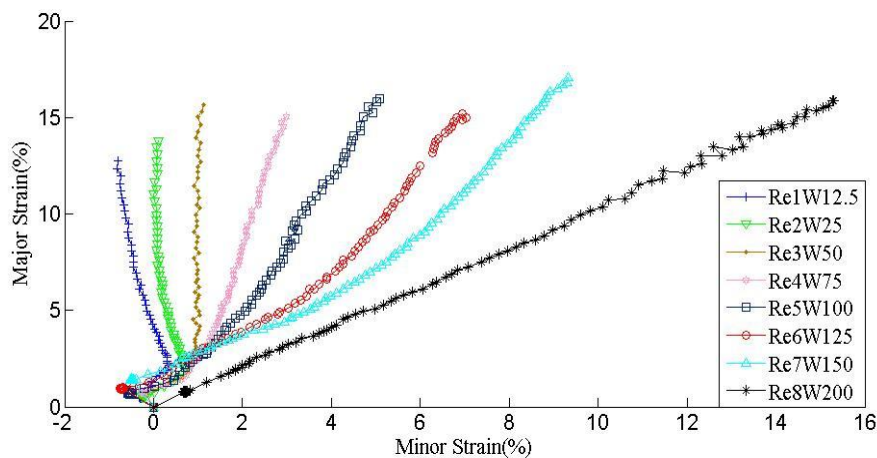


**Figure 3.** Pole strain evolution for different samples under stretch forming condition

It is noticeable that during all stages of deformation, the pole of the widest sample exhibited biaxial strain state, meaning major and minor strain ratio remained constant throughout the deformation, while thinner samples acted differently. At first they experienced shear deformation, followed by plain strain to biaxial strain state and afterwards they followed their main path of deformation depending on their size. This can be observed more clearly from figure 4. This behavior could be explained by considering stamping procedure applied in this experiment and observing tool-blank interactions during different stage of deformation. Tightening the blanks in the fixture equipped with a lock-ring caused the samples to be stretched prior to application of stamping press. This pre-stretch condition was recorded by the ARAMIS system, by taking pictures prior and posterior to tightening the samples in the die. The related pre-stretch strains for different geometries are presented in table 2.

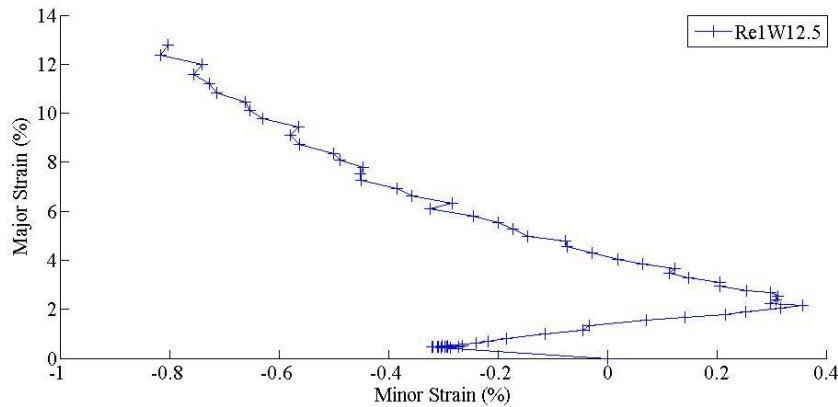


**Figure 4.** strain path change of thinnest sample during deformation stages

Sample	Minor Strain (%)	Major Strain (%)
Re1W12.5	-0.3	0.45
Re2W25	-0.19	0.53
Re4W75	-0.27	0.76
Re5W 200	0.68	0.73

**Table 2.** pre-stretch strains after fixing the blanks in the die

Evidently, the first part of the pole strain behavior is due to the effect of pre-stretch or locking effect. This path change is not noticeable in the bigger samples as they experienced a lot more strain before failure which de-accentuate the effect of pre-stretch strain. Justification of the second part of the pole evolution behavior will be feasible by considering contact interaction between blank and the punch during different stages of deformation. In the initial stages of deformation, the punch and blank contacted upon a very small circular area which caused a local deformation experienced by the sheets. Material outside this region acted as a fixed boundary. Therefore, the material inside contact region experienced biaxial stretch condition. This is evident in the second part of the pole evolution diagrams. By further penetration of the punch, more material got in contact with the tool, causing the whole sample to deform under actual boundary condition, thus following the final strain evolution.

### 3.3 Pre-failure strain conditions

During deformation of the samples, strain state of different surface points of the specimens might follow different paths: for some surface points, major to minor strain ratio remained constant, while for others it changed drastically during deformation. Strain ratio distributions for some of the samples at room temperature are demonstrated in Figures 5-8. It can be observed that surface points of Specimen Re1W12.5 have mostly experienced uniaxial strain state by distributing around a very small area in that region. Points of Re2W25 exhibiting a slight shift toward the plain strain state. Existence of relatively small amount of material in these two specimens has caused the identical deformation behavior. As the samples become wider, their surface points exhibit a more diverse strain state. This could be explained by existence of different areas on the surface each with a different forming and local boundary conditions causing diverse modes of deformation ranging from uniaxial strain state to biaxial strain state. Obviously, the minor strain window becomes wider in bigger samples. Thus, for a given major strain, the related pre-failure minor strain will cover a bigger envelope. *This clearly exhibit a better formability characteristic for this class of material compared to metals which offer a narrower strain envelope.*

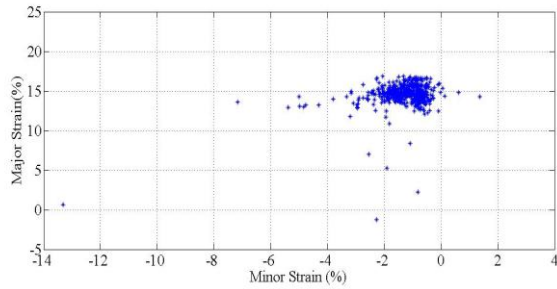


Figure 5. FLD of Re1W12.5

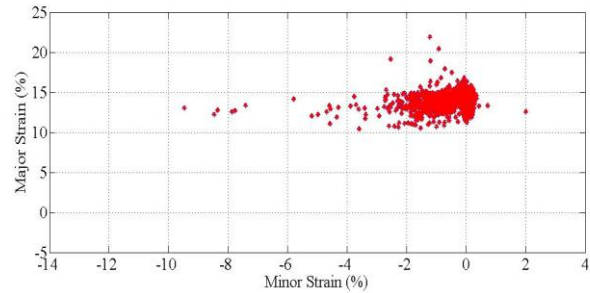


Figure 6. FLD of Re2W25

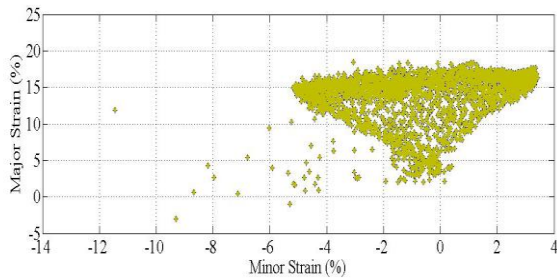


Figure 7. FLD of Re4W75

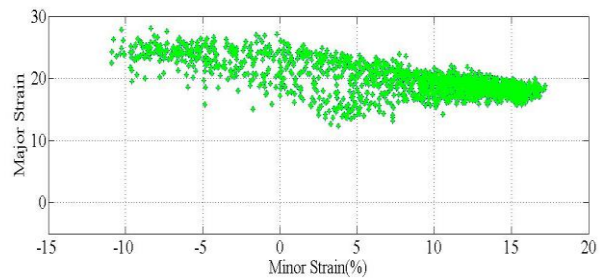


Figure 8. FLD of Re8W200

#### 4 Conclusions

The experimental work undertaken in this research comprised of stretch forming of different rectangular samples made of SRPP at room temperature. Wide strain envelope of SRPP during room temperature stretch forming proves its superior formability compared to metals. It promises remarkable energy saving in production accompanied by considerable weight reduction in products if metallic parts are substituted with this material. SRPP does not exhibit necking prior to the failure. Experimental results indicate that FLD comprises of two regions: Failed and non-failed regions. Therefore, in order to safely design parts and products out of this material, its behavior should be fully understood. The ARAMIS system is only able to track strains evolution on the surface. In order to predict the overall material behavior, an FEM code should be developed and utilized in conjunction with the ARAMIS outputs. This would be part of future studies

#### References

- [1] Suong D.G., Stephen V.H., Tsai W. Composite Materials Design and Application. CRC Press, Florida (2003).
- [2] Lamers E.A.D. Shape distortions in fabric reinforced composite products due to processing induced fibre reorientation., PhD Thesis, University of Twente (2004).
- [3] Brown K.A., Brooks R., Warrior N.A. Characterizing the Strain Rate Sensitivity of the Tensile Mechanical Properties of a Thermoplastic Composite. *Jom*, **61**, pp. 43-46 (2009).
- [4] Launay J., Gilles H., Duong Ahn V., Boisse P. Experimental analysis of the influence of tensions on in plane shear behaviour of woven composite reinforcements. *Composites Science and Technology*, **68**, pp. 506-515 (2008).
- [5] Abot J.L., Gabbai R.D., Harsley K. Effect of woven fabric architecture on interlaminar mechanical response of composite materials:an experimental study. *Journal of Reinforced Plastics and Composites*, **30**, pp. 2003-2014 (2011).

- [6] Cabrera N. O., Reynolds C. T., Alcock B., Peijs T. Non-isothermal stamp forming of continuous tape reinforced all-polypropylene composite sheet. *Composites Part A: Applied Science and Manufacturing*, **39**, pp. 1455-1466 (2008).
- [7] Lee J.H., Vogel J.H., Rhee K.Y. An analysis of stretch forming of thermoplastic composites. *Polymer Composites*, **23**, pp. 442-453 (2002).
- [8] Lim T.C., Ramakrishna S., Shang H.M. Axisymmetric sheet forming of knitted fabric composite by combined stretch forming and deep drawing. *Composites Part B: Engineering*, **30**, pp. 495-502 (1999).
- [9] tenThije R. H. W., Akkerman R., Ubbink M., van der Meer L. A lubrication approach to friction in thermoplastic composites forming processes. *Composites Part a-Applied Science and Manufacturing*, **42**, pp. 950-960 (2011).
- [10] Chen, Q., Boisse, P., Park C., Saouab A., Breard J. Intra/inter-ply shear behaviors of continuous fiber reinforced thermoplastic composites in thermoforming processes. *Composite Structures*, **93**, pp. 1692-1703 (2011).
- [11] Abbassi F., Elfaleh I., Mistou S., Zghal A., Fazzini M., Djilali T. Experimental and numerical investigations of a thermoplastic composite (carbon/PPS) thermoforming. *Structural Control & Health Monitoring*, **18**, pp. 769-780 (2011).
- [12] Zhu B., Yu T.X., Zhang H., Tao X.M. Experimental investigation of formability of commingled woven composite preform in stamping operation. *Composites Part B-Engineering*, **42**, pp. 289-295 (2011).
- [13] Keeler S.P. Automotive Sheet Metal Formability, American Iron and Steel Institute, Report AU89-1 (1989).
- [14] Sexton A., Cantwell W.J., Kalyanasundaram S. Stretch forming studies on a fibre metal laminate based on a self-reinforcing polypropylene composite. *Composite Structures*, **94**, pp. 431-437 (2012).
- [15] Mosse L., Cantwell W.J., Cardew-Hall M.J., Compston P., Kalyanasundaram S. The Effect of process temperature on the formability of fibre-metal laminates, *Composites Part A: Applied Science and Manufacturing*, **36**, pp. 1158-1166 (2005)
- [16] Mosse L., Cantwell W.J., Cardew-Hall M.J., Compston P., Kalyanasundaram S. A study of the effect of process variables on the stamp forming of rectangular cups using fibre-metal laminate systems, *Advanced Materials Research*, **68**, pp. 649-656 (2005).
- [17] Mosse L., Cantwell W.J., Cardew-Hall M.J., Compston P., Kalyanasundaram S. The development of a finite element model for simulating the stamp forming of fibre-metal laminates, *Composite Structures*, **75**, pp. 298-304 (2006).
- [18] Mosse L., Cantwell W.J., Cardew-Hall M.J., Compston P., Kalyanasundaram S. Stamp forming of Polypropylene based fibre-metal laminates: The effect of process variables on formability, *journal of materials processing technology*, **172**, pp. 163-168 (2006).
- [19] Morrow C., DharMalingam S., Venkatesan S., Kalyanasundaram S. *Stretch Forming Studies on Thermoplastic Composites*, ACAM 6, Perth, Australia (2010).